Journal of
*Composites Science*

MDPI

*Article*

# Thermal Characteristics Enhancement of AN/Mg/NC Composite Using Activated Carbon/Cobalt Oxide as Highly Effective Catalytic Additive

**Zhanerke Yelemessova [1,2,*], Symbat Kydyrbekova [1,2] and Ayan Yerken [2]**

[1] Institute of Combustion Problems, Almaty 050012, Kazakhstan; kydyrbekova.sn@gmail.com
[2] Faculty of Chemistry and Chemical Technology, Al-Farabi Kazakh National University, Almaty 050040, Kazakhstan; yerken.ayan@gmail.com
* Correspondence: zh.yelemessova@gmail.com

**Abstract:** Our study examined the potential of using activated carbon/nanosized cobalt oxide (AC-$Co_3O_4$) as a new catalytic additive to improve the efficiency of the parent ammonium nitrate/magnesium/nitrocellulose (AN/Mg/NC) composite. These findings demonstrate a significant improvement in the thermal characteristics of AN/Mg/NC/AC-$Co_3O_4$ compared to the initial AN/Mg/NC. Raman spectra confirmed the multilayered nature of AC. Fourier-transform infrared spectroscopy (FTIR) analysis confirmed the presence of cobalt oxide in the synthesized additive. Differential scanning calorimetry (DSC) revealed the catalytic effect of AC-$Co_3O_4$ on the AN/Mg/NC composite, resulting in the reduction in the decomposition peak temperature ($T_{max}$) from 277.4 °C (for AN/Mg/NC) to 215.2 °C (for AN/Mg/NC/AC-$Co_3O_4$). Thermal gravimetric analysis (TG) determined the overall mass losses (%) for AN/Mg/NC (70%), AN/Mg/NC/AC (75%), and AN/Mg/NC/AC-$Co_3O_4$ (80%). This analysis highlights the significant role of AC-$Co_3O_4$ in enhancing the energy release during decomposition. Moreover, the use of the differential thermogravimetric (DTG) technique demonstrated the two-step decomposition pathways attributed to the multi-component system. Finally, the combustion tests under the pressure of 3.5 MPa validated the catalytic efficiency of the AC-$Co_3O_4$ additive, which enhanced the burning rate ($r_b$) of the AN/Mg/NC/AC-$Co_3O_4$ composite from 10.29 to 19.84 mm/s compared to the initial AN/Mg/NC composite. The advantageous nature of the AN/Mg/NC/AC-$Co_3O_4$ composite with a lowered decomposition temperature can be applied in rocket propulsion systems, where the precise control of combustion and ignition processes is crucial.

**Keywords:** AN/Mg/NC composite; activated carbon; nanosized $Co_3O_4$; combustion; burning rate



**Citation:** Yelemessova, Z.; Kydyrbekova, S.; Yerken, A. Thermal Characteristics Enhancement of AN/Mg/NC Composite Using Activated Carbon/Cobalt Oxide as Highly Effective Catalytic Additive. *J. Compos. Sci.* **2023**, *7*, 471. https://doi.org/10.3390/jcs7110471

Academic Editor: Francesco Tornabene

Received: 16 September 2023
Revised: 26 October 2023
Accepted: 10 November 2023
Published: 11 November 2023



## 1. Introduction

Ammonium nitrate (AN), as a commercially available chemical compound, is extensively utilized as an oxidizing part of civil explosives [1]. The interest in AN-based composites has grown due to their eco-friendly properties such as clean burning characteristics and low toxicity [2]. However, some limitations of AN such as weak ignitability, insufficient burning rate, and excessive hygroscopicity diminish its wide application in energetic materials (EMs) [3]. Consequently, the facile combustibility of AN could only be realized in conjunction with specific combustible elements [4]. As a result, scientists began to investigate the impact of various additives (for example, metal oxides, ferrites, etc.) on the combustion characteristics of AN-based composites [5,6]. Some additives have proven to be effective as catalysts in the thermal decomposition of AN-based EMs [7–9]. Moreover, researchers have also assessed the impact of nanomaterials as additives on the decomposition of AN-based compounds [10–12]. Since some carbon nanomaterials can enhance the thermal conductivity, heat release, and reactivity of EMs, the complexity of their production makes them less cost-effective.

In several investigations, the impact of activated carbon (AC) on the thermal decomposition of EM was investigated [13–15]. For instance, AC based on rice husk (RH) can be an alternative to expensive nanomaterials, fulfilling the requirements for EM [16–18]. As is known, RH-based AC is a type of activated carbon derived from the agricultural waste product known as rice husk. Due to its better adsorption characteristics, common availability, and sustainability, it has attracted growing interest in the last decade. RH-based AC possesses several advantages, such as being abundant and eco-friendly, contributing to waste reduction. It is an inexpensive material with a substantial specific surface, minimal ash content, high porosity, and low density. AC has distinctive properties that make it an excellent choice as a support for metal oxides and contribute to its suitability for catalytic applications [19].

In recent times, nanostructured transition metal oxides have garnered considerable attention as a subject of extensive investigation, covering both fundamental and applied aspects due to their unique physicochemical properties. In our earlier research [20], we focused on the effects of the activated carbon/copper oxide additive on the decomposition of the parent AN/Mg/NC composition. In our present research, we considered cobalt oxide ($Co_3O_4$) due to its potential catalytic activity, which originates from its unique structure, electronic properties, and reactive surface [21]. As is known, $Co_3O_4$ contains active sites on its surface, which can interact with molecules in the composite and assist in the formation of intermediate species [22]. These intermediate species, in turn, decrease the reaction activation energy barriers, thus increasing the total reaction rate. The novelty of our research focuses on investigating the effect of $Co_3O_4$ inclusions such as AC-$Co_3O_4$ additives on the thermal characteristics of the initial AN/Mg/NC composite for promising applications in rocket propulsion systems.

Energetic materials, particularly those used in rocket propulsion systems, demand the precise control of their thermal characteristics. The decomposition and combustion properties of these materials are crucial for their performance and safety. The primary objectives of this research are as follows: (1) to investigate the impact of AC and nanosized cobalt oxide ($Co_3O_4$) inclusions on the temperature characteristics of the parent AN/Mg/NC composite, (2) to analyze the decomposition kinetics of the AN/Mg/NC/AC-$Co_3O_4$ composite using thermal analyses, and (3) to evaluate the catalytic properties of $Co_3O_4$ in AN/Mg/NC/AC-$Co_3O_4$.

## 2. Materials and Methods

### *2.1. Materials*

AN ($NH_4NO_3$, Sigma Aldrich (St. Louis, MO, USA), ACS reagent grade, ≥98%) was used as an oxidizer in the AN/Mg/NC composite. Magnesium (Mg, Sigma Aldrich, ≥99%) with a powder particle size of 0.06–0.30 mm was used as the fuel. Nitrocellulose (NC) served as an energy binder with a degree of nitration (12.5%) and with a purity of 96%. Rice husk-based activated carbon (RH-based AC) was synthesized in the laboratory. Cobalt oxide ($Co_3O_4$, Sigma Aldrich, nano powder <50 nm, 99.5% trace metals basis) was mechanically incorporated onto the external layer and microscopic openings of AC through planetary milling.

### *2.2. Methods and Equipment*

Synthesis of AC. Based on carbonized RH, AC was synthesized in a steel reactor under inert atmosphere. After carbonization, AC was immersed in a KOH solution to eliminate the by-product ($SiO_2$). Further, the obtained solution was decanted to remove the base, and the AC-containing material was placed into the reactor for activation (900 °C). In the next step, the obtained AC underwent a series of washing cycles with distilled water (approximately 20 cycles) to reach a pH value of 7. These processes culminated in the production of AC with a high specific surface area of ~3000 $m^2/g$ (by BET analysis) and an absorption capacity of ~360 mL/g (by methylene blue).

Equipment. The mass of the components was defined using a Shimadzu AY220 analytical balance (Shimadzu Corporation, Kyoto, Japan). To determine the surface structure of the obtained AC, the scanning electron microscope Quanta 200i 3D equipped with an energy dispersive X-ray analysis (EDAX) system (FEI Company, Hillsboro, OR, USA) was used. FTIR spectra of AC, $Co_3O_4$, and AC-$Co_3O_4$ were obtained using a Nicolet 5700 spectrophotometer (Thermo Fischer Scientific, Waltham, MA, USA). The Raman spectrum of AC was recorded using the probe-scanning microscope Integra Spectra (NT-MDT Spectrum Instruments, Tempe, AZ, USA). The morphology of AC-$Co_3O_4$ was examined using the JEM-2100 transmission electron microscope (JEOL Inc., Peabody, MA, USA).

Composite Sample Preparation. Figure 1 illustrates the steps involved in sample preparation. The synthesis of AC-$Co_3O_4$ involved the mechanical incorporation of cobalt oxide nanoparticles onto the external layer and microscopic openings of AC using a planetary milling process lasting 15 min. The resultant mixture underwent vacuum drying for a period of 24 h. All components, with the exception of the readily available magnesium, in the AN/Mg/NC and AN/Mg/NC/AC composites underwent a 24 h vacuum drying process. Additionally, based on the chosen ratios, the various components were measured by weight. The components obtained were subjected to a grinding process lasting 15 min. Magnesium was introduced into the crushed components and underwent a process of dry mixing in a mortar to achieve homogeneity in accordance with the specified ratios. For the chamber setup burning tests, the specimens were compacted into cylindrical tablets measuring 6 mm in diameter and 10 mm in length using a hydraulic press at a pressure of 5 MPa.

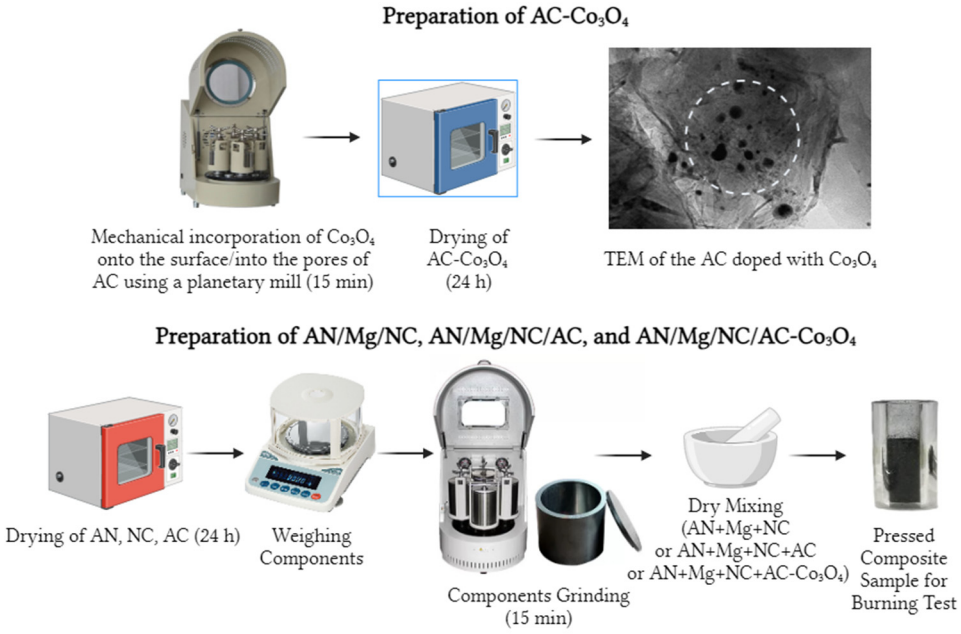


**Figure 1.** Preparation procedures for the AC-$Co_3O_4$, AN/Mg/NC, AN/Mg/NC/AC, and AN/Mg/NC/AC-$Co_3O_4$ composites.

Combustion Characteristics Measurements. The sample burning tests were conducted in a nitrogen-filled combustion chamber setup. The ignition of a sample was initiated by a nichrome wire, applying the required electric current voltage and pressures in the combustion chamber ranging from 1 to 3.5 MPa. To observe and record the sample burning process, the chamber setup was equipped with a viewport. To record the burning process, a special high-speed video camera (MotionXtraHG-100 K, Redlake MASD LLC, San Diego, CA, USA) with a frame rate of 1010 fps/1504 × 1128 pixel resolution was utilized. The linear burning rate of the sample was determined by analyzing the recorded videos from ignition to complete burnout, expressed in mm/s through linear regression. The calculation accuracy was approximately ±0.01 mm. Each combustion experiment was repeated three

times to estimate the average burning rate. Figure 2 illustrates the combustion chamber setup and the equipment utilized for the sample combustion tests under pressure.

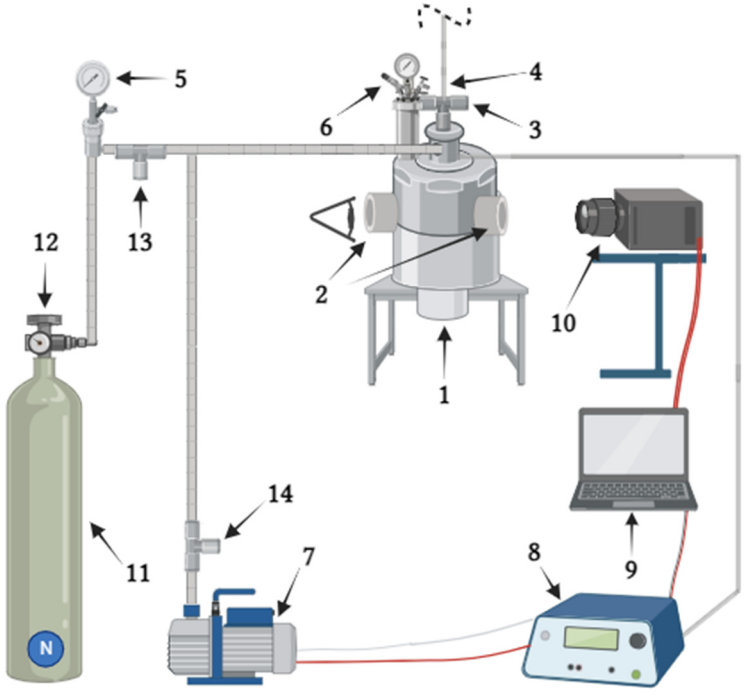


**Figure 2.** High-pressure experimental chamber setup for sample combustion test: 1—sample holder; 2—viewing window; 3—exit valve; 4—exhaust line; 5—pressure gauge; 6—pressure gauge; 7—vacuum pump; 8—power supply; 9—PC; 10—video recorder; 11—gas; 12—valve; 13—shut-off valve; 14—overlap valve.

The applied pressure during the combustion of a sample plays a substantial role in its burning rate ($r_b$) according to Saint Robert's/Vieille's law [23]. This empirical relationship (Equation (1)) offers valuable insights into the intricate aspects of combustion behaviour and kinetics:

$$r_b = r_o + a \cdot P^n \quad (1)$$

In Equation (1), the variable $r_b$ denotes the linear burning rate in millimeters per second (mm/s), while $r_o$ represents the initial burning rate constant. The burning rate coefficient is denoted by $a$, and the pressure exponent is denoted by $n$. Both $a$ and $n$ are empirical parameters that cannot be predicted theoretically. Equation (1) allows for the correlation of the linear burning rate ($r_b$) with pressure $P$ in megapascals (MPa), enabling its application across a range of operating conditions.

## 3. Results

### *3.1. Characterization of AC-$Co_3O_4$ Additive: Physicochemical Properties*

Figure 3 illustrates the morphological characteristics and elemental analysis of activated carbon (AC) and activated carbon with cobalt oxide ($Co_3O_4$). The micrograph in Figure 3a provides a detailed view of rice husk-based activated carbon (RH-based AC), revealing a distinct honeycomb pattern consisting of interconnected cells and rounded spaces. This unique structure enhances the material's exceptional qualities and is crucial for its applications, as it represents a highly porous system with interconnected storage units [24]. The extensive porosity also facilitates the distribution of metal oxide particles, making it valuable for composite materials. In Figure 3b, the Raman spectrum of the AC sample shows the intensity ratio of the G and D bands (ID/IG = 0.63). This ratio confirms the multilayered nature of the AC and indicates the presence of defects or disorder, which can impact its properties and reactivity. Understanding these structural aspects is essential

for optimizing the performance of activated carbon in various applications, including catalysis and energy storage.

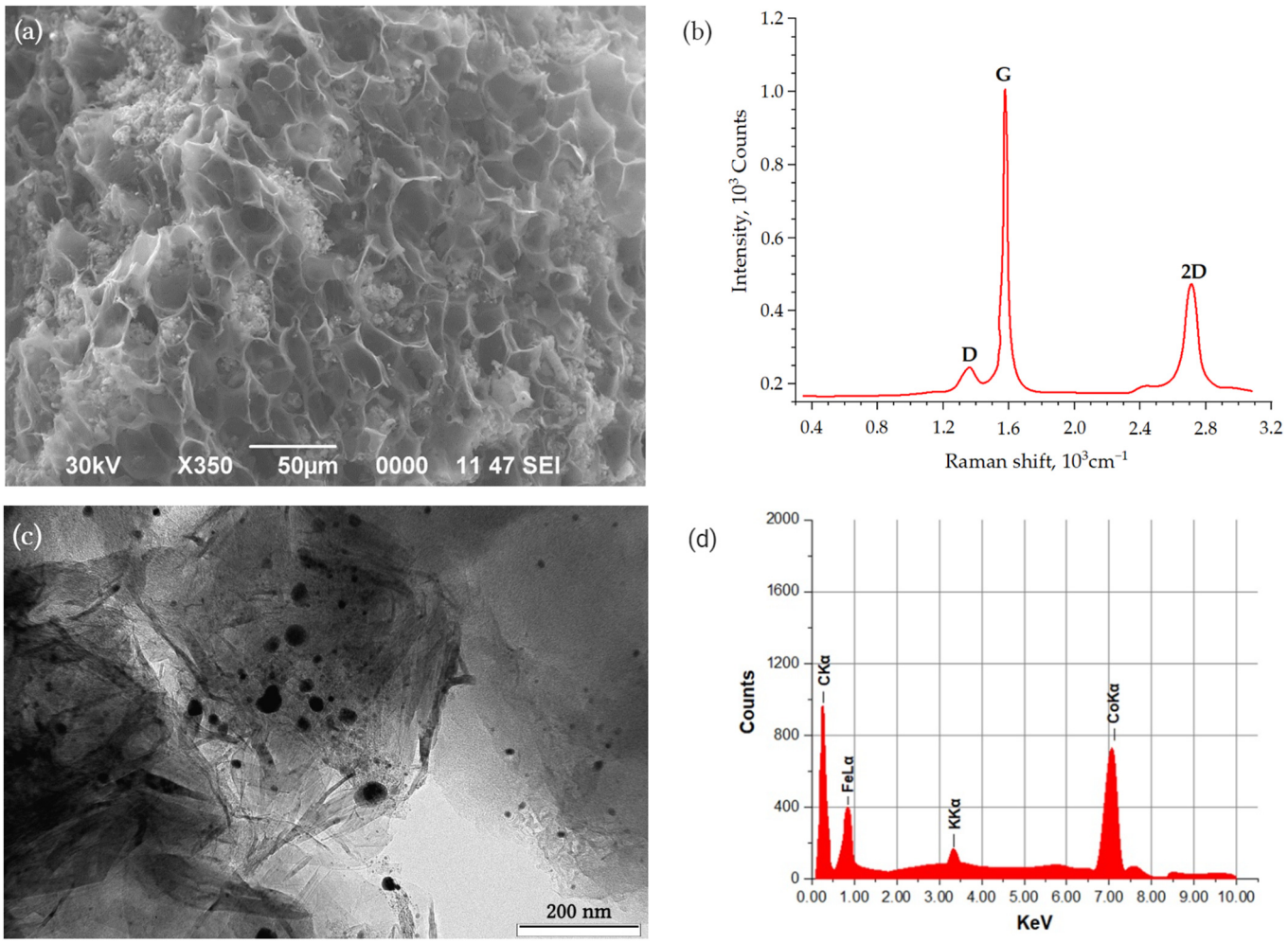


**Figure 3.** Morphological characterization and elemental analysis: (**a**) SEM of AC; (**b**) Raman of AC; (**c**) TEM of AC with $Co_3O_4$; (**d**) EDX of AC with $Co_3O_4$.

Moving to Figure 3c, the examination of the structure of AC reinforced with $Co_3O_4$ particles is a crucial aspect of our research and was meticulously carried out using transmission electron microscopy (TEM). The intricacies of this analysis are visually depicted in Figure 3c, which provides a compelling illustration of the noticeable integration of cobalt oxide particles within the matrix of AC. The incorporation of $Co_3O_4$ particles into the AC matrix is significant as it imparts distinct properties and functionalities to the resulting AN/Mg/NC/AC-$Co_3O_4$ composite. In Figure 3c, the presence of cobalt oxide particles within the structure of AC can be observed. $Co_3O_4$ is widely recognized for its catalytic activity, which has the potential to enhance the performance of AC in various applications. The coexistence of these two materials within the composite structure could lead to synergistic effects, resulting in improvements in adsorption capacity, catalytic properties, and thermal stability. These enhancements in the characteristics of the composite offer promising opportunities for its utilization across diverse technological and industrial domains. Figure 3d presents the outcomes of the Energy Dispersive X-ray Spectroscopy (EDX) analysis of the AC-$Co_3O_4$ additive (note: the oxygen signal was excluded to avoid cluttering the graph). The presence of certain amounts of potassium and iron on the AC surface is attributed to the AC production techniques, which involve chemical activation with various active reagents in metal containers.

### 3.2. FTIR Study of AC-$Co_3O_4$ Additive

The utilization of Fourier-transform infrared spectroscopy (FTIR) analysis has been employed to validate the existence of cobalt oxide within the AC matrix. This particular technique is frequently utilized to ascertain the chemical composition of various materials, including the inclusion of additives such as cobalt oxide in composites. By examining the FTIR spectra of AC, $Co_3O_4$, and AC-$Co_3O_4$, it becomes possible to identify the corresponding functional groups and chemical bonds that are present (see Figure 4).

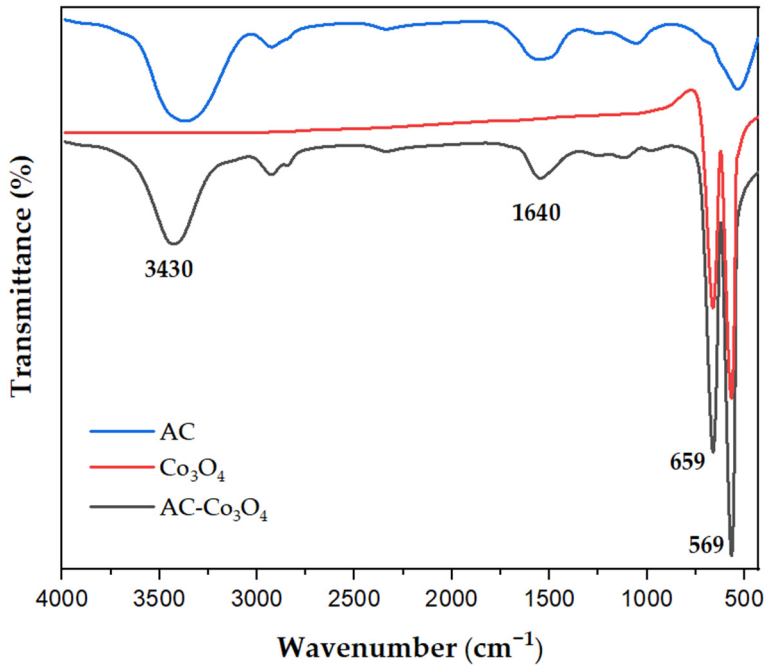


**Figure 4.** FTIR spectra of AC, $Co_3O_4$, and AC-$Co_3O_4$.

In accordance with previous studies [25], the O-H stretching vibration typically occurs within the range of 3200–3600 $cm^{-1}$ and is indicative of the presence of water molecules. These water molecules can originate from absorbed moisture in the surrounding environment or from hydroxyl (OH) groups on the surface of the material. The absorption band at 3430 $cm^{-1}$ is a distinctive feature associated with water-related vibrations. The peak observed at 1640 $cm^{-1}$ in the FTIR spectrum can be attributed to aromatic C=C bonds, which are commonly associated with graphitic structures found in activated carbon. Furthermore, the presence of cobalt oxide ($Co_3O_4$) in the AC-$Co_3O_4$ additive is supported by the two prominent absorptions at 659 and 569 $cm^{-1}$.

### 3.3. Thermal Decomposition Characteristics by DSC-TG

The thermal analysis technique known as differential scanning calorimetry (DSC) offers a prompt and efficient method for examining the thermal ignition properties of EMs. Figure 5 illustrates the DSC curves obtained from the AN/Mg/NC, AN/Mg/NC/AC, and AN/Mg/NC/AC-$Co_3O_4$ composites, with a heating rate of $\beta$ = 5 K/min, under a nitrogen atmosphere.

Figure 5 demonstrates the DSC curves for AN/Mg/NC, AN/Mg/NC/AC, and AN/Mg/NC/AC-$Co_3O_4$. The decomposition of the AN/Mg/NC composite (red dash curve) is characterized by two-stage exothermic reactions. The first exothermic peak occurs at $T_{max}$ = 201.3 °C (corresponds to the thermal decomposition of NC) with heat release of 2.1 mW/mg. The second exothermic peak appears at $T_{max}$ = 277.4 °C, (corresponds to the decomposition of AN) with heat release of 5.2 mW/mg. Moreover, an initial small heat absorption peak may be attributed to the polymorphic transition of AN, accompanied by a weak endothermic peak, which might be related to water evaporation.

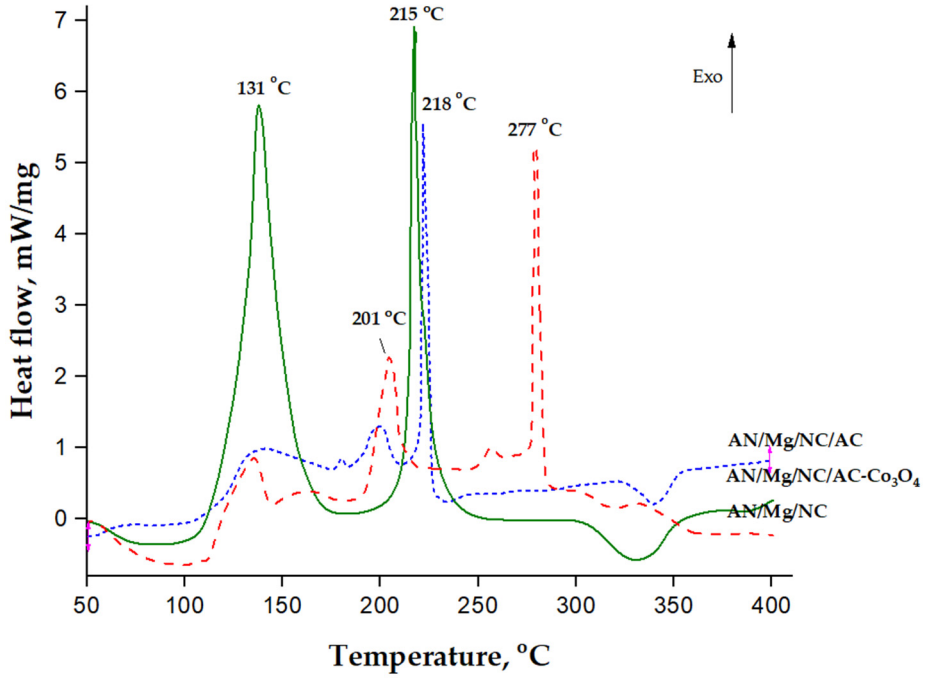


**Figure 5.** DSC analysis of AN/Mg/NC, AN/Mg/NC/AC, and AN/Mg/NC/AC-$Co_3O_4$ measured at β = 5 K/min.

The 5% inclusion of AC (blue dash curve) significantly altered the thermal behavior of the AN/Mg/NC/AC composite. The second peak experiences a decrease to $T_{max}$ = 218.2 °C (with heat release of 5.5 mW/mg) in comparison with the parent AN/Mg/NC composite with $T_{max}$ = 277.4 °C (with heat release of 5.2 mW/mg).

The 5% inclusion of AC-$Co_3O_4$ (green curve), a similar thermal decomposition process for the AN/Mg/NC/AC-$Co_3O_4$ composite, is observed. The addition of AC-$Co_3O_4$ to the parent composite AN/Mg/NC results in a faster decomposition rate of the new AN/Mg/NC/AC-$Co_3O_4$. The decomposition temperature of AN/Mg/NC/AC-$Co_3O_4$ becomes 215.2 °C (with heat release of 6.9 mW/mg) in comparison with 277.4 °C for AN/Mg/NC (with heat release of 5.2 mW/mg).

Figure 6 presents a comprehensive depiction of the thermogravimetric (TG) and derivative thermogravimetric (DTG) profiles acquired from the three distinct samples under investigation. The experimental procedure involved subjecting the samples to controlled heating in a nitrogen environment, with a heating rate (β) of 5 K/min. In Figure 6a, the TG curves of the three samples demonstrate a consistent trend of gradual mass reduction, spanning the temperature range of 40 to 500 °C. It is worth noting that the data highlight notable variations in the overall mass losses observed among the different compositions.

The AN/Mg/NC sample, represented by the red curve, demonstrates a mass loss of approximately 70% *w*/*w*. However, the addition of activated carbon in AN/Mg/NC/AC, as indicated by the blue curve, leads to an elevated mass loss of about 75% *w*/*w*. Remarkably, the composition of AN/Mg/NC/AC-$Co_3O_4$ (represented by the green curve) exhibits the highest mass loss, approximately 80% *w*/*w*. The substantial variation observed highlights the significant influence of these additives on the process of thermal decomposition. Figure 6b illustrates the derivative thermogravimetric (DTG) curves, providing a more comprehensive analysis of the decomposition mechanisms. The presented curves depict an intricate and multistep decomposition pathway that is characterized by the occurrence of more than three distinct processes. The complexity and multi-component composition of the composite materials being studied can be attributed to these processes. Upon the completion of the TG analysis, the residues that remain consist mainly of unreacted metal (Mg), the catalyst, and the condensed decomposition products of nitrocellulose

(NC) and ammonium nitrate (AN). Notably, the TG curves of the AN/Mg/NC/AC and AN/Mg/NC/AC-$Co_3O_4$ samples exhibit substantial variations when compared to the reference sample (AN/Mg/NC). These differences signify that the presence of activated carbon and cobalt oxide promotes more comprehensive decomposition, leading to relatively fewer residues. This observation holds significant importance, as it signifies the effectiveness of these additives in optimizing the decomposition process and improving the thermal properties of the composite materials.

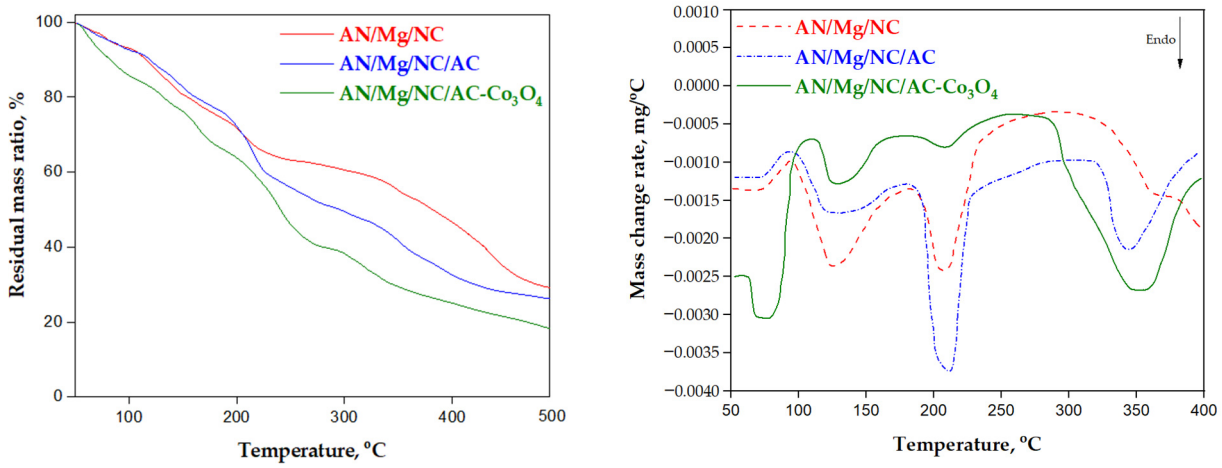


**Figure 6.** (**a**)TG curves of the AN/Mg/NC, AN/Mg/NC/AC, and AN/Mg/NC/AC-$Co_3O_4$ in a nitrogen medium. (**b**) DTG curves of AN/Mg/NC, AN/Mg/NC/AC, and AN/Mg/NC/AC-$Co_3O_4$ in a nitrogen medium.

### *3.4. Comparison of Combustion Characteristics: AN/Mg/NC vs. AN/Mg/NC/AC-$Co_3O_4$*

For the successful application of energetic materials, it is crucial to have control over the linear burning rate and the value of the pressure exponent. The value of n must be less than 0.6 for rocket propellants and higher than 1.0 for gun propellant applications [8] (p. 29). Figure 7 presents the results of combustion experiments for the following composites: (a) AN/Mg/NC (mass ratio 60/35/5), (b) AN/Mg/NC/AC (mass ratio 60/30/5/5), and (c) AN/Mg/NC/AC-$Co_3O_4$ (mass ratio 60/30/5/5), conducted at an initial pressure ($p_o$) of 3.5 MPa under inert environment.

Figure 7a depicts the propagation of the combustion wave in the AN/Mg/NC composite without any additives. The burning rate ($r_b$) for this material is measured to be 10.29 mm/s under an initial pressure of 3.5 MPa. The combustion process is characterized by the emission of bright light, which can be attributed to the vigorous burning of magnesium. In Figure 7b, the addition of AC to the AN/Mg/NC composite has a negligible impact on its combustion behavior. The linear burning rate remains relatively unchanged, reaching a value of 17.55 mm/s at the same applied pressure of 3.5 MPa. It is possible that the presence of AC promotes the reaction, leading to an improvement in the burning characteristics of the composite. The advancement of the combustion front is accompanied by a significant emission of light. Figure 7c shows the AN/Mg/NC composite sample with the addition of AC-$Co_3O_4$, which achieves the highest burning rate ($r_b$). The inclusion of this catalyst enhances the combustion behavior of the composite, resulting in an increased burning rate of 19.84 mm/s under an initial pressure of 3.5 MPa.

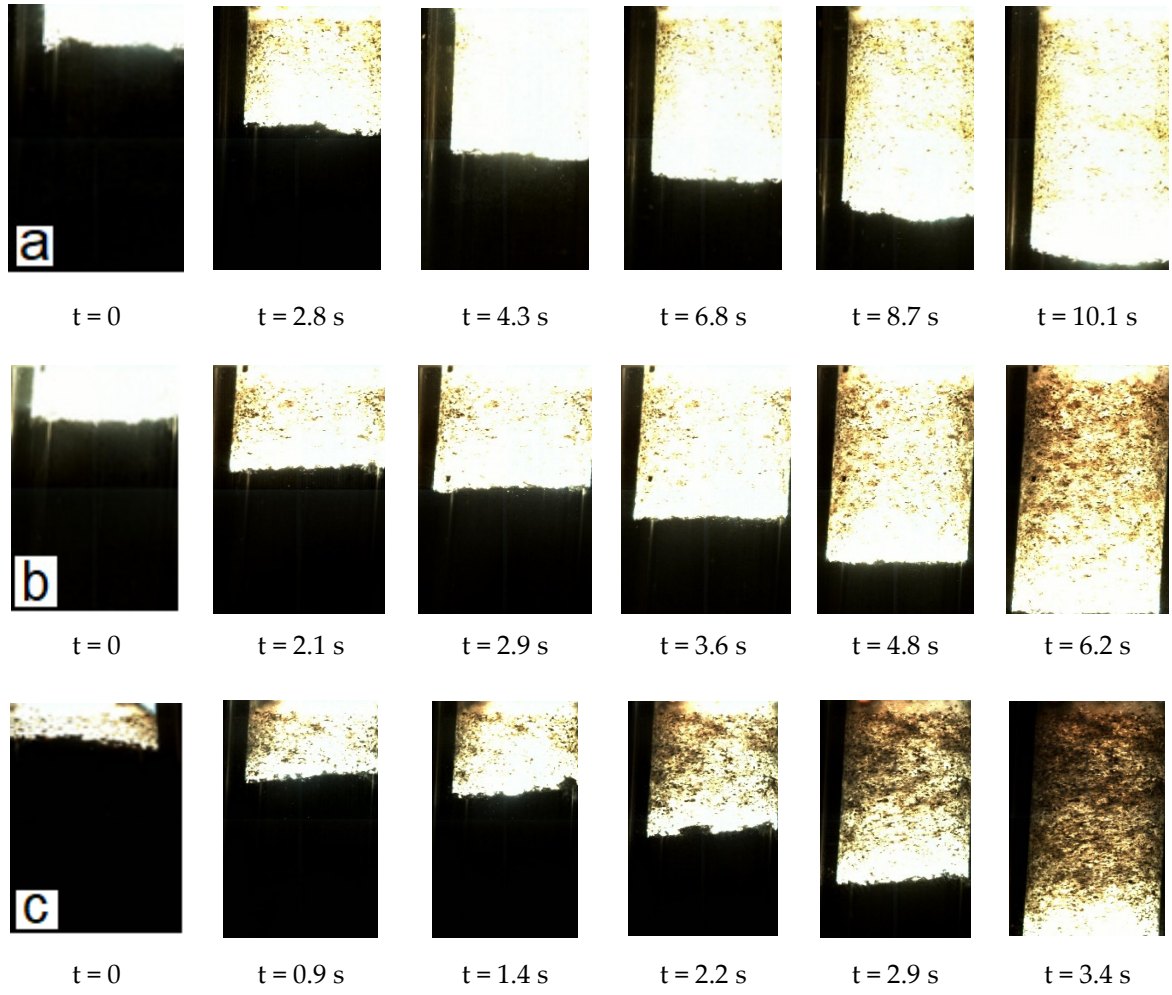


**Figure 7.** Combustion wave propagation (at 3.5 MPa) of the following composites: (**a**) AN/Mg/NC, (**b**) AN/Mg/NC/AC, and (**c**) AN/Mg/NC/AC-$Co_3O_4$.

The combustion wave propagation of the new AN/Mg/NC/AC-$Co_3O_4$ composite is illustrated in Figure 8, with initial pressures of 1, 2, and 3 MPa in a nitrogen medium. It is evident that an increase in the initial pressure results in an augmented velocity of the combustion wave. At 1 MPa (Figure 8a), the combustion process demonstrates uniformity, characterized by a slow burning rate of 10.00 mm/s and a limited release of visible gases. As the initial pressure is raised to 2 (Figure 8b) and 3 MPa (Figure 8c), the burning rate of the composite is further enhanced to 14.76 and 16.87 mm/s, respectively.

Figure 9 shows a comparison of the linear burning rates under the pressure of 3.5 MPa for three composites: AN/Mg/NC, AN/Mg/NC/AC, and AN/Mg/NC/AC-$Co_3O_4$. The AN/Mg/NC/AC-$Co_3O_4$ composite has the highest burning rate, reaching 19.84 mm/s at an initial pressure of 3.5 MPa. Both the AN/Mg/NC and AN/Mg/NC/AC composites exhibit low burning rates and pressure exponents ($n$ = 0.53–0.42), indicating a low susceptibility to mechanical and shock impacts. The addition of AC-$Co_3O_4$ improves the combustion process of the AN/Mg/NC/AC-$Co_3O_4$ composite, leading to a burning speed of 19.08 mm/s, a high burning rate coefficient (a = 11.36), and a low-pressure exponent value ($n$ = 0.42).

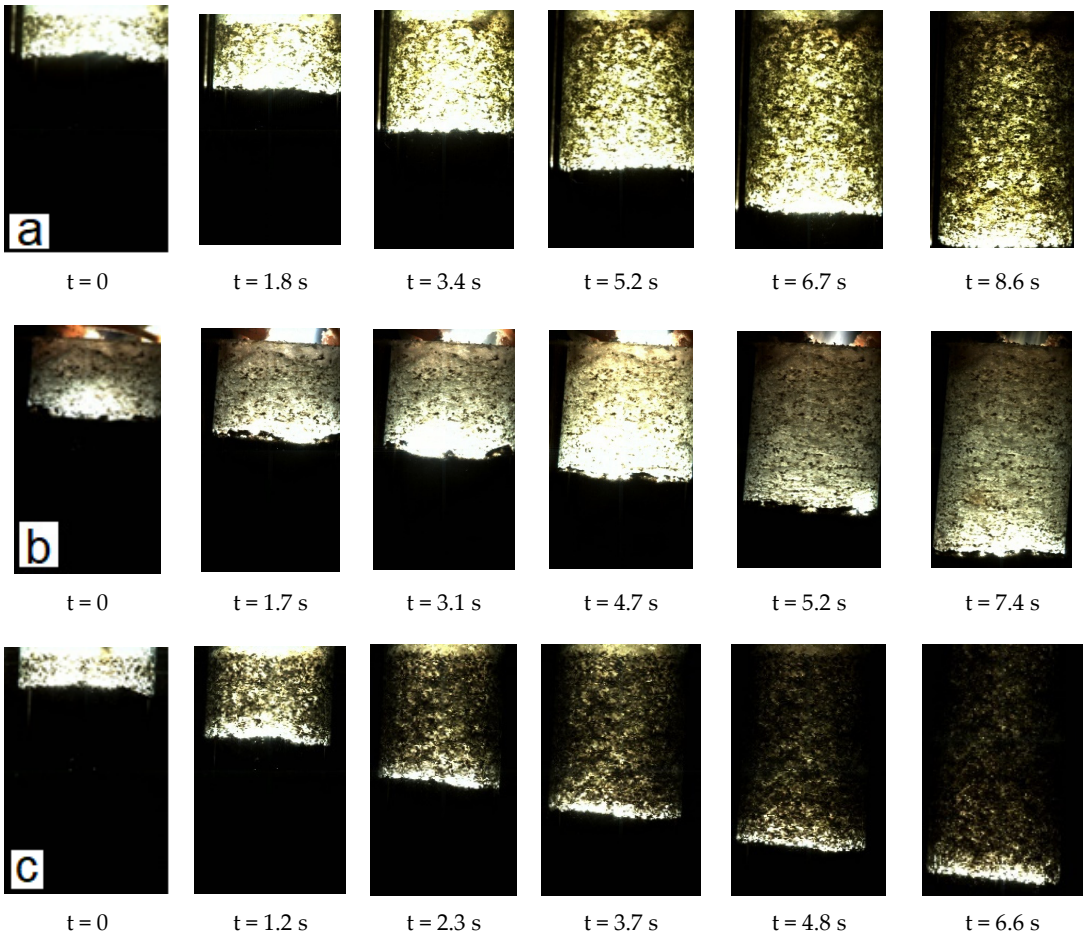


**Figure 8.** Combustion wave propagation of AN/Mg/NC/$Co_3O_4$ at initial pressure ($p_o$): (**a**) 1 MPa, (**b**) 2 MPa, and (**c**) 3 MPa.

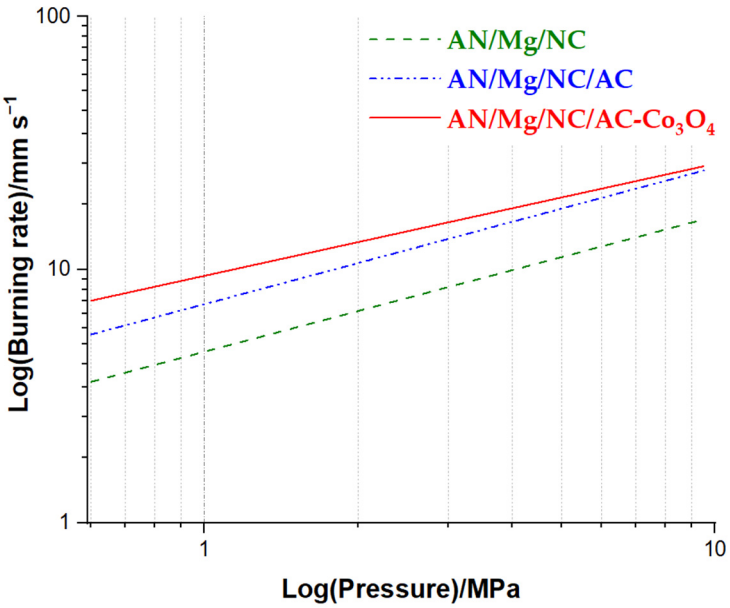


**Figure 9.** Influence of initial pressure on the burning rates of AN/Mg/NC, AN/Mg/NC/AC, and AN/Mg/NC/AC-$Co_3O_4$ composites.

### 3.5. Catalytic Mechanism of the AC-$Co_3O_4$ Effect

The internal mechanism of the catalytic effect of AC-$Co_3O_4$ on heat release may involve several factors. Firstly, the AC-$Co_3O_4$ additive acts as a catalyst and reduces the activation energy needed for the decomposition of the composite. This means that at a lower temperature (131 °C vs. 201 °C), a higher burning rate of 19.84 mm/s vs. 10.29 mm/s (Figure 7c) in comparison with the initial AN/Mg/NC can occur, resulting in increased heat release from 2.1 to 5.3 mW/mg (Figure 5). Secondly, the $Co_3O_4$ component of AC-$Co_3O_4$ may provide catalytic sites that facilitate the decomposition of AN/Mg/NC. Cobalt oxide may serve as a platform where chemical reactions can take place more readily, leading to a faster release of energy. Thirdly, the inclusion of AC-$Co_3O_4$ may have the potential to enhance the rate of the decomposition reaction, which implies that the AN/Mg/NC/AC-$Co_3O_4$ composite undergoes more efficient conversion into products, resulting in the release of energy. Fourthly, the synergistic effects may arise from the combination of activated carbon (AC) and cobalt oxide ($Co_3O_4$). The porous nature of AC facilitates a significant increase in the available surface area, enabling enhanced interaction between reactants and $Co_3O_4$. This, in turn, promotes the catalytic activity. Fifthly, AC may possess adsorption properties that enable the absorption of reaction intermediates and products, thereby decreasing their concentration and promoting the progress of the reaction towards completion with increased heat release.

In essence, the catalytic effect of AC-$Co_3O_4$ on heat release is a complex interplay of these factors, encompassing lower activation energy, catalytic sites provided by $Co_3O_4$, enhanced reaction rates, synergistic interactions, and adsorption properties of AC. This comprehensive understanding of the internal mechanisms involved sheds light on the significant improvements in thermal properties observed in the AN/Mg/NC/AC-$Co_3O_4$ composite. Table 1 provides the comparative thermal analysis results for AN/Mg/NC, AN/Mg/NC/AC, and AN/Mg/NC/AC-$Co_3O_4$.

**Table 1.** Comparison of thermal analysis results of AN/Mg/NC, AN/Mg/NC/AC, and AN/Mg/NC/AC-$Co_3O_4$ composites.

| Composite | Initial Peak Temperature /Heat Release | Main Peak Temperature /Heat Release | Total Heat Release * (mW/g) | Burning Rate ($r_b$) at 3.5 MPa | Flame Brightness Level at 3.5 MPa |
|---|---|---|---|---|---|
| AN/Mg/NC | 201.3 °C<br>2.1 mW/g | 277.4 °C<br>5.2 mW/g | 73.2 | 10.29 mm/s | Exceptionally high |
| AN/Mg/NC/AC | 132 °C<br>1.0 mW/g | 218.2 °C<br>5.5 mW/g | 86.3 | 17.55 mm/s | Average |
| AN/Mg/NC/AC-$Co_3O_4$ | 131 °C<br>5.3 mW/g | 215.2 °C<br>6.9 mW/g | 92.7 | 19.84 mm/s | Low |

* According to the calculated area under the DSC curve.

According to the data presented in Table 1, the incorporation of AC-$Co_3O_4$ as an additive into the resulting AN/Mg/NC/AC-$Co_3O_4$ composite results in a significant improvement in the combustion properties of the final AN/Mg/NC/AC-$Co_3O_4$ composite. AC-$Co_3O_4$ serves as a catalytic additive in the composite of AN/Mg/NC/AC-$Co_3O_4$, effectively enhancing its burning rate through the regulation of the decomposition pathways of the oxidizer (AN) and binder (NC) [26]. Additionally, the AN/Mg/NC/AC-$Co_3O_4$ composite may exhibit the enhanced combustion efficiency due to the significant specific surface area, abundant surface centers for reactions, porosity, and excellent heat transfer properties of the activated carbon (AC) [27]. The incorporation of AC-$Co_3O_4$ into the AN/Mg/NC composite enables the regulation of both the linear burning rate and pressure exponent values in the resulting AN/Mg/NC/AC-$Co_3O_4$ composite.

## 4. Discussion

The current research provides a key understanding of the influence of activated carbon/cobalt oxide additive on the decomposition (combustion) behavior of the AN/Mg/NC composite. The effect of AC-$Co_3O_4$ reveals a substantial impact on AN/Mg/NC decomposition. The reduction in onset decomposition temperature and increased heating rate indicates the catalytic role of activated AC-$Co_3O_4$ in enhancing thermal decomposition. Table 2 presents the thermal decomposition characteristics of some AN-based composites investigated in a previous study within the field.

**Table 2.** Thermal decomposition characteristics of some composites.

| Composite | Onset Temperature, °C | Peak Temperature, °C | Max. Heat Flow, mW/g | References |
|---|---|---|---|---|
| AN + ZnFO | - | 166 | 0.061 | [28] |
| AN + MgFO | - | 164 | 0.036 | [28] |
| AN/$CuFe_2O_4$ | 244 | 307 | - | [28] |
| AN/CB24 | 185 | - | 3.400 | [29] |
| AN/Mg/NC/AC-$Co_3O_4$ | 108 | 215 | 6.900 | Current study |

Data from Table 2 demonstrate a comparative analysis of the thermal decomposition properties of some AN-based composites, highlighting the progress made in our ongoing research in comparison to a prior study conducted in the same field. Our research has yielded substantial advancements in certain thermal characteristics.

The findings hold significant implications for the field of energetic materials, offering potential applications in the advancement of propellants and explosives. The improved thermal characteristics, such as reduced decomposition temperature and increased heat release rate, could lead to more efficient and effective propulsion systems. The aforementioned phenomenon can significantly influence the defense and aerospace sectors, where the accurate regulation of combustion and ignition procedures holds utmost importance.

The use of catalytic additives such as AC-$Co_3O_4$ to enhance the thermal characteristics of energetic materials can contribute to increased safety and reduced environmental impacts. By reducing the decomposition temperature, there is the potential to mitigate the occurrence of the unintended ignition or accidental detonation of these materials. This is a matter of utmost importance in both military and civilian contexts.

The research conducted in this study has potential applications in the chemical industry, specifically in areas related to the synthesis of compounds that necessitate the accurate management of exothermic reactions. Understanding how catalytic additives influence energy release can aid in the design of safer manufacturing processes and the development of novel chemical compounds.

This study places emphasis on the integration of activated carbon derived from sustainable sources such as agricultural waste, in conjunction with metal oxide. This approach presents potential avenues for the adoption of more ecologically sound production methods, which aligns with the growing emphasis on sustainability and reducing the environmental footprint in various industries. The findings presented in the article can provide a solid basis for future research and advancement in the field of energetic materials. Researchers and industries may be inclined to explore innovative additives and composite materials in order to enhance the efficiency of these fundamental substances.

## 5. Conclusions

In this research, the potential of application of activated carbon/nanosized cobalt oxide (AC-$Co_3O_4$) as a novel catalytic additive to improve the performance of the initial ammonium nitrate/magnesium/nitrocellulose (AN/Mg/NC) was investigated. Our com-

prehensive analysis reveals a substantial improvement in the thermal characteristics of the AN/Mg/NC/AC-$Co_3O_4$ composite compared to the unmodified AN/Mg/NC composite.

Raman spectroscopy confirmed the multilayered structure of the activated carbon (AC). Additionally, Fourier-transform infrared spectroscopy (FTIR) analysis corroborated the presence of cobalt oxide in the synthesized AC-$Co_3O_4$ additive, confirming its successful integration into the composite structure. Differential scanning calorimetry (DSC) elucidated the catalytic effect of AC-$Co_3O_4$ on the AN/Mg/NC composite. This phenomenon led to a significant decrease in the decomposition peak temperature ($T_{max}$) from 277.4 °C (for the unmodified AN/Mg/NC) to 215.2 °C (for the new AN/Mg/NC/AC-$Co_3O_4$).

Furthermore, the overall mass losses (%) for each composite were quantified using thermal gravimetric analysis (TG), with AN/Mg/NC/AC-$Co_3O_4$ demonstrating the highest mass loss (80%). The presence of AC-$Co_3O_4$ plays a crucial role in augmenting the energy release during decomposition, thereby positioning it as a promising additive for enhancing combustion efficiency.

The application of the differential thermo-gravimetric (DTG) technique enabled us to elucidate the intricate, two-step decomposition pathways inherent in the multi-component system. These findings offer crucial insights into the process of decomposition and the role played by the AC-$Co_3O_4$ additive in facilitating these pathways.

Finally, the catalytic efficiency of the AC-$Co_3O_4$ additive was validated through combustion tests conducted under a pressure of 3.5 MPa. The burning rate ($r_b$) of the AN/Mg/NC/AC-$Co_3O_4$ composite exhibited significant improvement, reaching a value of 19.84 mm/s, in contrast to the initial AN/Mg/NC composite (10.29 mm/s).

In conclusion, this study highlights the significant potential of the AN/Mg/NC/AC-$Co_3O_4$ composite due to its reduced decomposition temperature and enhanced combustion rate. The aforementioned attributes render it a highly promising material for applications in rocket propulsion systems, wherein the precise calibration of combustion and ignition procedures holds utmost significance. The catalytic additive AC-$Co_3O_4$ presents promising opportunities for enhancing the performance of energetic materials, thereby facilitating safer and more efficient applications across diverse domains.

Future research directions could be directed towards investigating the stability and long-term effects of these additives on the characteristics of the composite material. Such investigations have the potential to provide valuable insights into the durability and practical feasibility of these additives. Exploring the potential synergistic effects of different catalysts or optimizing their loading amounts has the potential to enhance the performance of the composite material. Future research endeavors can utilize these valuable insights to advance the progress in the field of high-performance composite materials, with a specific emphasis on tailoring their combustion properties.

**Author Contributions:** Conceptualization, Z.Y.; methodology, Z.Y. and S.K.; software, A.Y.; validation, Z.Y. and S.K.; formal analysis, Z.Y. and S.K.; investigation, Z.Y.; resources, Z.Y.; data curation, A.Y.; writing—original draft preparation, Z.Y.; writing—review and editing, Z.Y.; visualization, Z.Y.; supervision, Z.Y.; project administration, Z.Y.; funding acquisition, Z.Y. All authors have read and agreed to the published version of the manuscript.

**Funding:** This research is funded by the Science Committee of the Ministry of Science and Higher Education of the Republic of Kazakhstan, grant number AP13268793.

**Data Availability Statement:** The data presented in this study is available upon request from the corresponding author.

**Acknowledgments:** We extend our gratitude to the eminent Kazakhstani scientists Mansurov, Lesbayev, Kamunur, and Atamanov for their invaluable contributions, guidance, and unwavering support throughout the research. Their expertise, insights, and encouragement have been instrumental in shaping the direction and enhancing the quality of this research.

**Conflicts of Interest:** The authors declare no conflict of interest.

## References


1. Oxley, J.C.; Kaushik, S.M.; Gilson, N.S. Thermal decomposition of ammonium nitrate-based composites. *Thermochim. Acta* **1989**, *153*, 269–286. [CrossRef]
2. Jos, J.; Mathew, S. Ammonium nitrate as an Eco–friendly oxidizer for composite solid propellants: Promises and challenges. *Crit. Rev. Solid State Mater. Sci.* **2016**, *42*, 470–498. [CrossRef]
3. Yang, M.; Chen, X.; Wang, Y.; Yuan, B.; Niu, Y.; Zhang, Y.; Liao, R.; Zhang, Z. Comparative evaluation of thermal decomposition behavior and thermal stability of powdered ammonium nitrate under different atmosphere conditions. *J. Hazard. Mater.* **2017**, *337*, 10–19. [CrossRef]
4. Sinditskii, V.P.; Egorshev, V.Y.; Levshenkov, A.I.; Serushkin, V.V. Ammonium nitrate: Combustion mechanism and the role of Additives. *Propellants Explos. Pyrotech.* **2005**, *30*, 269–280. [CrossRef]
5. Kamunur, K.; Jandosov, J.M.; Abdulkarimova, R.G.; Hori, K.; Yelemessova, Z.K. Combustion study of different transitional metal oxide based on AN/MgAl composites gas generators. *Eurasian Chem.-Technol. J.* **2017**, *19*, 341. [CrossRef]
6. Dave, P.N.; Sirach, R. Thermal decomposition study of ammonium nitrate in the presence of nickel-zinc ferrite additive. *Catal. Commun.* **2023**, *177*, 106639. [CrossRef]
7. Han, Z.; Sachdeva, S.; Papadaki, M.I.; Mannan, M.S. Ammonium nitrate thermal decomposition with additives. *J. Loss. Prev. Process. Ind.* **2015**, *35*, 307–315. [CrossRef]
8. Yan, Q.-L.; Gozin, M.; Zhao, F.-Q.; Cohen, A.; Pang, S.-P. Highly energetic compositions based on functionalized carbon nanomaterials. *Nanoscale* **2016**, *8*, 4799–4851. [CrossRef]
9. Hanafi, S.; Trache, D.; Meziani, R.; Boukeciat, H.; Tarchoun, A.F.; Abdelaziz, A.; Mezroua, A. Thermal decomposition and kinetic modeling of HNTO/AN-based composite solid propellant in the presence of GO-based nanocatalyst. *Fire Phys. Chem.* **2022**, *2*, 315–322. [CrossRef]
10. Reid, D.L.; Russo, A.E.; Carro, R.V.; Stephens, M.A.; LePage, A.R.; Spalding, T.C.; Petersen, E.L.; Seal, S. Nanoscale additives tailor energetic materials. *Nano Lett.* **2007**, *7*, 2157–2161. [CrossRef]
11. Dave, P.N.; Sirach, R. Thermal decomposition of ammonium nitrate (AN) in the presence of the optimized nano-ternary transition metal ferrite $CoNiZnFe_2O_4$. *Energy Adv.* **2022**, *1*, 690–696. [CrossRef]
12. Song, X.; Wang, Y.; Song, D.; An, C.; Wang, J. Catalysis of a nanometre solid super acid of $SO_4^{2-}/TiO_2$ on the thermal decomposition of ammonium nitrate. *Nanomater. Nanotechnol.* **2016**, *6*, 23. [CrossRef]
13. Stankovich, S.; Dikin, D.A.; Dommett, G.H.; Kohlhaas, K.M.; Zimney, E.J.; Stach, E.A.; Piner, R.D.; Nguyen, S.T.; Ruoff, R.S. Graphene-based composite materials. *Nature* **2006**, *442*, 282–286. [CrossRef] [PubMed]
14. Miyake, A.; Kobayashi, H.; Echigoya, H.; Ogawa, T. Combustion and ignition properties of ammonium nitrate and activated carbon mixtures. *Int. J. Energ. Mater. Chem. Propuls.* **2009**, *8*, 411–419. [CrossRef]
15. Zhang, T.; Gao, X.; Li, J.; Xiao, L.; Gao, H.; Zhao, F.; Ma, H. Progress on the application of graphene-based composites toward Energetic Materials: A Review. *Def. Technol.* **2023**; (*Article in Press*). [CrossRef]
16. Mansurov, Z.A.; Atamanov, M.K.; Elemesova, Z.; Lesbaev, B.T.; Chikradze, M.N. New nanocarbon high-energy materials. *Combust. Explos. Shock Waves* **2019**, *55*, 402–408. [CrossRef]
17. Atamanov, M.K.; Amrousse, R.; Hori, K.; Kolesnikov, B.Y.; Mansurov, Z.A. Influence of activated carbon on the thermal decomposition of hydroxylammonium nitrate. *Combust. Explos. Shock Waves* **2018**, *54*, 316–324. [CrossRef]
18. Mansurov, Z.A.; Amrousse, R.; Hori, K.; Atamanov, M.K. Combustion/decomposition behavior of HAN under the effects of nanoporous activated carbon. In *Innovative Energetic Materials: Properties, Combustion Performance and Application*; Pang, W., DeLuca, L.T., Gromov, A., Cumming, A., Eds.; Springer: Singapore, 2020; pp. 211–230. [CrossRef]
19. Zhou, C.; Wang, Y. Recent progress in the conversion of biomass wastes into functional materials for value-added applications. *Sci. Technol. Adv. Mater.* **2020**, *21*, 787–804. [CrossRef]
20. Atamanov, M.; Yelemessova, Z.; Imangazy, A.; Kamunur, K.; Lesbayev, B.; Mansurov, Z.; Yue, T.; Shen, R.; Yan, Q.-L. The catalytic effect of CuO-doped activated carbon on thermal decomposition and combustion of AN/Mg/NC composite. *J. Phys. Chem. C* **2019**, *123*, 22941–22948. [CrossRef]
21. Chen, J.; Wu, X.; Selloni, A. Electronic structure and bonding properties of cobalt oxide in the spinel structure. *Phys. Rev. B* **2011**, *83*, 245204. [CrossRef]
22. Gu, D.; Jia, C.-J.; Weidenthaler, C.; Bongard, H.-J.; Spliethoff, B.; Schmidt, W.; Schüth, F. Highly ordered mesoporous cobalt-containing oxides: Structure, catalytic properties, and active sites in oxidation of carbon monoxide. *J. Am. Chem. Soc.* **2015**, *137*, 11407–11418. [CrossRef]
23. Maggi, F.; DeLuca, L.T.; Bandera, A.; Subith, V.S.; Annovazzi, A. Burn-rate measurement on small-scale rocket motors. *Def. Sci. J.* **2006**, *56*, 353–367. [CrossRef]
24. Kwiatkowski, J.F. *Activated Carbon: Classifications, Properties and Applications*; Nova Science Publishers: New York, NY, USA, 2012.
25. Nassar, M.Y.; Ahmed, I.S. Hydrothermal synthesis of cobalt carbonates using different counter ions: An efficient precursor to nano-sized cobalt oxide ($Co_3O_4$). *Polyhedron* **2011**, *30*, 2431–2437. [CrossRef]
26. Luo, Q.; Ren, T.; Shen, H.; Zhang, J.; Liang, D. The thermal properties of nitrocellulose: From thermal decomposition to thermal explosion. *Combust. Sci. Technol.* **2017**, *190*, 579–590. [CrossRef]
27. Yelemessova, Z.K.; Imangazy, A.M.; Tulepov, M.I.; Mansurov, Z.A. Energetic Metal–organic frameworks: Thermal behaviors and combustion of nickel oxide (II) based on activated carbon compositions. *J. Eng. Phys. Thermophys.* **2021**, *94*, 804–811. [CrossRef]

28. Cabrera, A.F.; Torres, C.E.R.; Juncal, L.C.; Meyer, M.; Stewart, S.J. Effect of nanostructured ferrites $MFe_2O_4$ (M = Cu, Co, Mg, Zn) on the thermal decomposition of ammonium nitrate. *Appl. Energy Combust. Sci.* **2021**, *6*, 100026. [CrossRef]
29. Izato, Y.-I.; Miyake, A.; Date, S. Combustion Characteristics of Ammonium Nitrate and Carbon Mixtures Based on a Thermal Decomposition Mechanism. *Propellants Explos. Pyrotech.* **2013**, *38*, 129–135. [CrossRef]